Synthesis and application of silver nanoparticles as biocidal agent in polyurethane coating

M. Bechtold, A. Valério, A. A. Ulson de Souza, D. de Oliveira, C. V. Franco, R. Serafim, S. M. A. Guelli U. Souza

Abstract Nanostructured materials have become increasingly widespread, and in recent decades, the processing industries have shown a great interest in coating materials with antibacterial properties. In this research, the biocidal effect of silver nanoparticles in the water-soluble polyurethane paint composition was evaluated. Silver nanoparticles in the aqueous phase were prepared by chemical reduction at 500 ppm using polyvinyl alcohol. The material was characterized by UV–Vis, inductively coupled plasma mass spectrometry, dynamic light scattering, zeta potential, and transmission electron microscopy. The effect of silver nanoparticles in terms of yellowing and gloss variation was evaluated by a UV-B radiation test. Silver nanoparticles had no effect on the gloss and yellowing paint film. In addition, positive results were obtained for the protection and resistance against bacteria but not satisfactory resistance against fungi.

Keywords Antibacterial paints, Nanotechnology, Silver-based biocide, Coating

Introduction

The use of nanostructured materials has become increasingly widespread, and in recent decades, the processing industries have shown a great interest in coating materials with antibacterial properties.[1–4] Due to the wide variety of organic and inorganic molecules in the different types of coatings, a variety of microor-

ganisms can grow in these substrates if they find favorable environmental conditions.[5,6] Through inappropriate packaging and storage, microorganisms can affect the appearance and stability of the paint. Also, in the cured film, microorganisms can cause film discoloration, stains, biofilm formation, and even damage such as cracking and paint film disintegration.[2,7,8]

Several aspects should be considered in choosing a biocide for use in paint, such as a broad application spectrum, high efficiency in low amounts, easy handling and incorporation into the paint, good chemical stability, low toxicity, and no bioaccumulation.[5,9,10] The demand for coatings that repel microorganisms is growing. The largest amounts of paint biocides are consumed in the construction industry, particularly to produce interior and exterior paints that are formulated to provide protection against the growth of mold and mildew. Currently, however, the consumption of paint biocides is growing in other fields, including hospitals, nursing homes, medical applications, and the food and pharmaceutical industries, among others.[1,11–14]

Silver is a mineral extracted from the natural environment, and its antiseptic action has been known for millennia, but in the form of nanoparticles, it has a much larger surface contact and its properties are greatly increased.[5,15] Studies have demonstrated that silver can eliminate more than 650 pathogenic organisms showing a huge spectrum of activity. Moreover, silver in the form of nanoparticles is harmless to health and its production cost is extremely competitive.[16–18]

Thus, silver-based biocides are increasing in popularity. There is a growing interest in using this type of biocide in antimicrobial paints. However, the addition of these products in traditional paints can have some unwanted side effects including discoloration of the paint film, loss of brightness, and low stability.[5,19] As mentioned above, this research was carried out with the aim to produce and characterize biocide-based

M. Bechtold, A. Valério, A. A. Ulson de Souza,
D. de Oliveira, C. V. Franco, R. Serafim,
S. M. A. Guelli U. Souza (✉)
Department of Chemical and Food Engineering (EQA),
Federal University of Santa Catarina (UFSC),
Florianópolis, SC 88040-900, Brazil
e-mail: selene.souza@ufsc.br

silver nanoparticles, to verify the effect of this biocide in a waterborne polyurethane paint, and to evaluate the biocidal efficiency of silver nanoparticles, both in-can and in the cured film.

Materials and methods

Synthesis and characterization of silver nanoparticles (AgNPs)

AgNPs were synthesized by chemical reduction using sodium borohydride ($NaBH_4$) as a reducing agent and sodium citrate as a stabilizer, based on the methodology reported by Jana et al.[20] The synthesis was performed in an ice bath to reduce the velocity of the reactions and promote the formation of micelles. The borohydride was also previously cooled to prevent degradation. All solutions were prepared with ultra-pure water (Milli-Q grade) at 4°C. The $AgNO_3$ solution was added to the sodium citrate under vigorous stirring in a precooled beaker. The solution of $NaBH_4$ was then added to the beaker under agitation. The reduction of silver by $NaBH_4$ proceeded according to equation 1.

$$4Ag^+ + n\,BH_4^- + 3n\,H_2O \rightarrow 4Ag + n\,H_2BO_3^- + 4n\,H^+ + 2n\,H_2$$

$$(1)$$
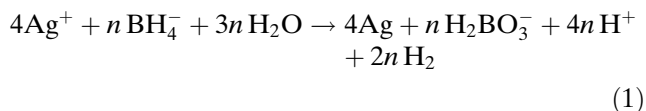
The reagents were used to synthesize a solution with 500 ppm. To enhance the stability of the colloidal dispersions, polyvinyl alcohol (PVA) was added to the reaction medium. The real concentrations of the synthesized AgNPs dispersions were measured by inductively coupled plasma mass spectrometry (ICP-

MS) using a PerkinElmer SCIEX spectroscope. UV-visible spectra were recorded with a quartz cell (1 cm path length) using a Cary 50 Bio spectrophotometer to evaluate the size distribution and shape of the AgNPs. The zeta potential of the dispersions and the size distribution of the nanoparticles were measured by dynamic light scattering (DLS) on a Malvern Instruments Zetasizer Nano system. Transmission electron microscopy (TEM) using a JEM-1011 microscope was used to evaluate the shape, size distribution, and crystallinity of the AgNPs.

Polyurethane paint preparation

The polymer used to study the interaction with the AgNPs was a polyurethane system chosen because of its high light stability, chemical resistance, and hardness. A polyurethane system was formed from the reaction of the paint (polyol resin) and the crosslinker (polyisocyanate) agent, according to the reaction presented in equation 2.

$$-NCO \;+\; HO-R \;\longrightarrow\; -NH-C{\overset{\displaystyle O}{\underset{\displaystyle O-R}{<}}}$$

$$(2)$$

For the in-can preservation, a biocide based on BIT (1,2-benzisothiazolin-3-one) and a biocide based on IBPC (3-iodo-2-propynylbutylcarbamate) were used to evaluate the resistance of the cured films against fungi and bacteria. The formulations of the white polyol phase are presented in Table 1. The crosslinker agent, aliphatic polyisocyanate (90 wt%), and glycol ether acetate (10 wt%) were used for all paint (polyol phase) formulations.

Table 1: Formulations of polyol phase

Sample identification	Composition	% (v/v)
Negative control	Acrylic emulsion	70
	Concentrate of titanium dioxide	15
	Water	15
AgNP system	Acrylic emulsion	70
	Concentrate of titanium dioxide	15
	AgNP dispersion	15
Positive control: "in-can" preservation	Acrylic emulsion	70
	Concentrate of titanium dioxide	15
	Water	14.8
	Biocide based on BIT	0.2
Positive control: Resistance to fungi and bacteria	Acrylic emulsion	70
	Concentrate of titanium dioxide	15
	Water	14.5
	Biocide based on IBPC	0.5

UV-B radiation test

The test was performed in order to evaluate the effects of UV-B radiation on the cured film, such as changes in color (mostly yellowing) and gloss. The equipment used was a UV-B Comexim chamber, which fulfills the requirements of the ASTM G154/2004[21] and operates in interspersed cycles with 4 h under UV-B at 60°C and 4 h under condensation at 50°C. After this test, the specimens were removed from the chamber, rinsed with water, and dried with soft paper for subsequent evaluation of color and brightness.

To prepare the specimens for the UV-B radiation test, each coating (polyol phase) was mixed with the crosslinker in a ratio of 100 parts of the polyol phase to 10 parts of the crosslinker (w/w), using a 10% excess of NCO as normally used in industry. This excess is used in order to ensure that all the hydroxyl reacts with the isocyanate since some isocyanate reacts with water. To ensure perfect homogeneity, mechanical stirring was applied. The mixture was then left to stand for 15 min (induction time) before application, to allow prepolymerization of the components. The paints were applied, after the induction time, on degreased steel panels with a dry film layer of 30–40 μm. There were six specimens for each sample (three to be exposed for 360 h and three for 1500 h to UV-B radiation), and thus, the tests were performed in triplicate. The specimens were dried at room temperature (25°C and 50% relative humidity) and were left under these conditions for 7 days before the testing so that total crosslinking of the system could occur.

After exposure to UV-B radiation, the color changing of the specimens was measured by spectrophotometry using a Datacolor SF450X Spectraflash spectrophotometer. The illuminant used for testing was daylight D65. This analysis is widely used in the coating industry to evaluate variations in color after destructive tests. The gloss changing was measured by a BYK-Gardner glossmeter, with a light source (incandescent lamp), and photodetectors placed at an angle of 60º from the perpendicular plane of the specimen under testing were used according to ASTM D523.[22] Measurements were taken both in samples submitted for UV-B testing and in the control samples to evaluate the matting of the film after the destructive test.

Microbial content

The polyol samples were initially checked to assess the degree of contamination through plate streaking of Tryptic Soy Agar (TSA) for bacteria and Yeast Malt Extract Agar (YM), Malt Extract Agar (MA), Sabouraud Dextrose Agar (SDA), and Potato Dextrose Agar (PDA, adjusted to pH 3.5) for fungi and yeasts. The plates were incubated for a period of 24–48 h at 35°C for the bacteria detection.

The samples were also evaluated by transferring an aliquot with a sterile swab into culture tubes containing Tryptic Soy Broth (TSB). The tubes were incubated for 24 h at 35°C and then streaked on plates of TSA, which were incubated for 24–48 h at 35°C. The growth rate was ranked on a scale from 0 (no bacterial recovery) to 4 (heavy contamination), − (no growth), and + (growth), based on the number of colonies.

In-can preservation

The test was performed to determine the relative resistance of the applied paints on the container against the microorganisms according to ASTM D2574-94[23] with some modifications. The samples were inoculated with a pool of microorganisms containing *Pseudomonas aeruginosa* (ATCC 10145), *Enterobacter aerogenes* (ATCC 13048), and *Staphylococcus aureus* (ATCC 6538). The level of concentration for Challenge I was 10^9 CFU/g (colony-forming units per gram), 2.15×10^8 CFU/g for Challenge II, and 1.89×10^8 CFU/g for Challenge III.

The inoculated samples were shaken vigorously and incubated at 35°C throughout the test. At appropriate intervals, the presence of viable microorganisms was evaluated through the streaking of the samples on TSA plates with a sterile loop. The samples were incubated for 48 h at 35°C, and the degree of contamination was rated on a scale of 0 (no bacterial recovery) to 4 (heavy contamination). Any degree of growth (1–4) indicated that the sample was not adequately preserved against microorganisms.

Fungal resistance

The relative resistance of the coating films against fungi was carried out according to ASTM D5590.[24] The samples were prepared (100 parts of the polyol to 10 parts of the crosslinker—w/w) and applied on paper card squares (3.5×3.5 cm^2). These samples were evaluated after being leached with distilled water for 24 h and also without leaching. The specimens painted with the specific coatings were placed on the surface of plates containing Malt Agar and inoculated with a fungal suspension of *Aspergillus niger* (ATCC 6275) and *Penicillium funiculosum* (ATCC 11797). All the samples were tested in duplicate and incubated at 28°C with 85–90% humidity for 4 weeks. The fungal growth rate was evaluated weekly on a scale of 0 (no growth) to 10 (heavy growth).

Bacterial resistance

The antimicrobial activity and antimicrobial efficiency against bacteria on the coatings surface were evaluated according to JIS Z 2801:2000[25] with some modifications. *Escherichia coli* (ATCC 8739) and *Staphylococcus aureus* (ATCC 6538) were grown individually in TSB medium for 24 h, and the inoculum concentration

was adjusted to 10.[5,6] The samples were prepared (100 parts of the polyol phase to 10 parts of the crosslinker w/w) and applied to paper card squares (3.5×3.5 cm^2). Each bacterium was placed in a sterilized Petri dish and inoculated with 0.25 mL of the inoculum. The test inoculum was covered with a film to better spread the inoculum on the Petri dish. The test was performed after 0 and 24 h of contact, in which serial dilution was carried out according to the pour plate technique in order to observe a log increase or decrease to verify the effectiveness of the biocide added. The antimicrobial agent was estimated to be effective if the antimicrobial activity was > 2 calculated according to equation 3.

Antimicrobial activity

$$= \log(\text{negative control after 24 h/sample after 24 h})$$

$$(3)$$

Results and discussion

Synthesis and characterization of AgNPs

In this work, the dark color of the obtained dispersions suggests the formation of some nanoparticles agglomerates. According to Jin et al.,[26] AgNP dispersions which are completely free of agglomerates should have a light yellow color. Dispersions with a high concentration of agglomerates are turbid, but this effect was not observed in the dispersions prepared. The color depends on the dimensional and geometric properties of the particles with a direct effect on the plasmon resonance, according to the Mie theory, and a characteristic of the noble metal nanoparticles is the strong color of their colloidal dispersions.[27,28]

According to Table 2, a difference was observed between the theoretical (calculated reagents) and real

Table 2: Test results of AgNP dispersion characterization

Test	Characteristic	Results
ICP-MS	Real concentration (ppm)	487.3 ± 7.1
UV-Vis	Peak (nm)	394
	FWHM (nm)	45
	Asymmetry	0.5
TEM	Size distribution (nm)	37 (80%)
DLS	Size distribution (nm)	37 (85%)
		3 (15%)
Zeta potential	Conductivity (mS/cm)	1.88
	Distribution (mV)	$- 9$ (61%)
		$- 61$ (5%)
pH		8.5

AgNP concentration (ICP-MS analysis). For this case, the real concentration was lower than the theoretical concentration. The difference can be related to aggregation of AgNPs on the container walls.

Regarding the results obtained from the UV spectra, the maximum wavelength and bandwidth depend on the particle size, morphology, and composition during the measurements. The peaks are the result of a combination of absorption and light scattering due to interactions with the plasmonic field. Only a single plasmon band is expected in the absorption spectra of spherical nanoparticles, while anisotropic particles may form two or more plasmon bands depending on the different shapes of the nanoparticles, and according to Mie theory, silver particles smaller than 40 nm show a strong peak located in the region between 380 and 420 nm.[26,29]

Based on this theory, there was the formation of spherical AgNPs smaller than 40 nm with one band with a peak location at 394 nm. The symmetry of the band formed, calculated from the FWHH (full width at half height), is associated with the homogeneity of the particle size distribution. Symmetrical bands suggest a narrow distribution of particle sizes, and asymmetric bands suggest a wide distribution of sizes. According to the results obtained, the AgNPs dispersion showed a low asymmetry and consequently a narrow particle size. The DLS test and TEM histogram results (Table 2) corroborate with previous results, showing that the dispersion has an average particle size predominantly below 40 nm.

The magnitude of the zeta potential gives an indication of the potential stability of the colloidal system. If all the particles in suspension have a large negative or positive zeta potential, then they will tend to repel each other and there will be no tendency for the particles to agglomerate.[30] However, if the particles have low zeta potential values, then there will be no force to prevent the particles agglomerating and flocculating.[31] The general dividing line between stable and unstable suspensions is taken as either + 30 or − 30 mV. Particles with zeta potential values more positive than + 30 mV or more negative than − 30 mV are normally considered stable.[32] Some factors should be considered in the evaluation of zeta potential, and one of the most important factors is the pH of the dispersions.[33] Therefore, a zeta potential versus pH curve will be positive at low pH and lower or negative at high pH values. In this work, the pH of the dispersion was 8.5 and at this point, the zeta potential is negative, corroborating with the result obtained from the shift of the curve for negative zeta potential value.

TEM micrographs confirm the results obtained from the UV–Vis spectra discussed above with spherical AgNPs, which are predominantly smaller than 40 nm, as shown in Fig. 1. In the diffraction images, we can observe the formation of some rings, which is related to the polycrystalline particles. The spaces observed between the AgNPs can be attributed to the encapsulate (PVA) used during synthesis.
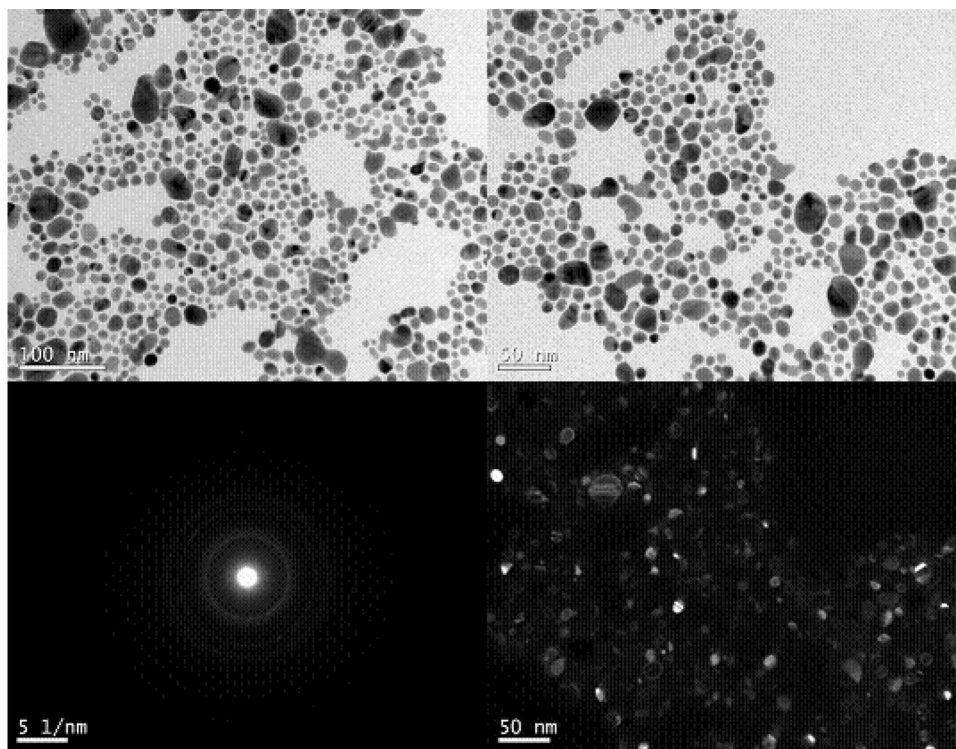
Fig. 1: TEM micrographs of polyurethane dispersion with AgNPs (500 ppm) using bright-field, dark-field, and diffraction techniques

To evaluate the stability of the AgNPs dispersion and in order to compare the result with the zeta potential, an additional ICP-MS test was carried out. On analyzing the variation in the AgNPs concentration from 487 to 420 ppm after 4 months, it can be stated that the steric stabilization generated by PVA was effective, as the zeta potential values (related to the electrostatic stabilization) of the dispersion indicate extreme instability of the system.

UV-B radiation test

Specimens were removed from the UV-B test chamber after 360 and 1500 h. The specimens were free of bubbles, cracking, or peeling areas on the coating. Gloss measurements were carried out before and after the exposure to UV-B radiation. The results for the average gloss value of the specimens applied with AgNP samples and the control (without AgNPs) were compared, as shown in Table 3. The tendency toward matting was the same in all situations, indicating that the AgNPs did not tend to modify the gloss of the coating.

Besides changing the gloss, another characteristic measured after the UV-B radiation test was the change in color by spectrophotometric analysis based on CIELAB color space. The spectra for the samples were obtained before and after the test to observe

Table 3: Average gloss of the specimens after UV-B radiation

UV-B radiation (h)	0	360	1500
Negative control (GU)	75	65	54
AgNP system (GU)	76	67	55

Table 4: Mean values for the *L*, *a*, and *b* scale of the samples against UV-B radiation time

UV-B radiation (h)	Sample	L	a	b
360	AgNP system	96.03	− 1.43	4.5
1500	AgNP system	96.13	− 1.38	4.1

Negative control: L = 96.88; a = − 1.08; b = 1.82

changes in these values, and the results for the specimens are presented in Table 4.

A strong tendency toward yellowing of the coatings formulated with AgNPs compared with the negative control can be noted from the results. The b results show that the control tends to blue, while the paint with AgNPs tends to yellow. This is a very negative result as yellowing is an undesirable consequence in the paint industry, especially when dealing with a

Table 5: Evaluation of microbial content

Sample	Culture medium					TSB enrichment
	TSA	MA	SDA	PDA	YM	TSA
Negative control	0	0	0	0	0	–
Positive control	0	0	0	0	0	–
AgNP system	0	0	0	0	0	–

Table 6: Determination of the relative resistance of the paint in the container to microorganism growth according to ASTM D2574

Sample	Challenge—"In-can"					
	Days					
	1 I	3	7 R	14 R	21	28
Negative control	0	3	2	2	1	1
Positive control	0	0	0	0	0	0
AgNP system	0	0	0	0	0	0

Microorganism growth level: 0 = no growth; 1 = early (1–9 colonies); 2 = low (10–99 colonies); 3 = moderate (> 100 colonies); 4 = high (no distinction between colonies)

Table 7: Relative resistance to fungal growth according to ASTM D5590

	Growth rate[a,b]							
	Not leached				Leached			
Week(s)	1	2	3	4	1	2	3	4
Negative control	9	10	10	10	9	10	10	10
Positive control	0	0	0	0	0	0	0	0
AgNP system	5	8	10	10	2	6	10	10

[a]Growth rate: 0 = complete absence of fungi; 10 = full fungal growth

[b]Inoculum *Aspergillus niger* (ATCC 6275) and *Penicillium funiculosum* (ATCC 11797)

polyurethane coating. Another change in the behavior with the addition of AgNPs is that the control tends to redden, while the AgNPs coating tends to become greenish (*a*). According to the *L* values, in all situations tested, the paint tends to darken.

Microbial content

The results for the evaluation of the microbial contamination of the paints are presented in Table 5. All samples showed a low growth level (0), an indication of free microbiological contamination before starting the tests.

The results for the determination of the relative paint resistance against microorganisms are reported in Table 6, where *I* indicates the day of inoculation and *R* the day of reinoculation, both performed before the inoculation streak. From the results, no microorganism growth in the samples with AgNPs was observed, confirming the effectiveness of the AgNPs in the tested concentration. Another observation is that the negative control, after 3 days of inoculation, showed a growth level of 3, with a decrease over the test time, showing that the paint studied is not suitable for the growth of colonies. This phenomenon may occur because some raw materials used in the formulation, such as the resin or pigment concentrate, contained a minimal amount of biocidal agents.

Table 8: Determination of the relative resistance to *Staphylococcus aureus* growth according to the JIS Z 2801:2000 method

Sample	Average number of viable cells of *Staphylococcus aureus* (CFU/mL)	Antimicrobial activity
Negative control (initial time)	3.3×10^5	–
Negative control (after 24 h)	2.1×10^4	–
Positive control (after 24 h)	< 10	> 4
AgNP system (after 24 h)	4.0×10^1	2.72

The results for the determination of the relative resistance against fungi are shown in Table 7. The samples with AgNPs showed very similar results to the negative control, suggesting that the AgNPs in the tested concentration were not enough to inhibit fungi growth in the cured films. Studies such as that reported by Panáček et al.[34] have demonstrated the efficiency of AgNPs against fungi. Thus, the results described above

Table 9: Determination of the relative resistance to *Escherichia coli* growth according to the JIS Z 2801:2000 method

Sample	Average number of viable cells of *Escherichia coli* (CFU/mL)	Antimicrobial activity
Negative control (initial time)	2.3×10^6	–
Negative control (after 24 h)	2.9×10^5	–
Positive control (after 24 h)	< 10	> 5
AgNP system (after 24 h)	2.7×10^2	3.03

could be attributed to an insufficient concentration of AgNPs in the coating film. It is known that fungi have much slower metabolisms than bacteria and therefore require higher concentrations of biocides to be inhibited.

The results for the determination of the relative resistance to bacterial growth are reported in Tables 8 and 9, and the effectiveness of the AgNPs is confirmed at the concentrations tested. The standard method considers that the sample tested is effective when the antimicrobial activity is ≥ 2 and the results for the test against the bacterium *Staphylococcus aureus* are very close to 2. This result suggests that the concentration of AgNPs in the samples is close to the minimum inhibitory concentration (MIC).[13,35,36]

Conclusions

The characterization tests showed the formation of spherical particles, mostly less than 40 μm, resulting in dispersions with dark coloration and the formation of few agglomerates. Regarding the stability of the dispersion synthesized, months after the preparation of nanoparticle dispersion, the concentration had not changed significantly, which suggests that the encapsulation effectively provided steric stabilization. On exposure to UV-B radiation, the photocatalytic effect on the AgNPs leads to yellowing of the coating film, an undesirable effect in the paint industry. In the microbiological assessments, the AgNPs demonstrated satisfactory performance in the in-can preservation tests (ASTM D2574-94) and resistance to bacteria in the dry film (JIS Z 2801). At the concentration used, the AgNPs were not efficient in terms of fungal resistance, yielding results very close to those obtained with the negative control. To achieve efficiency, higher doses of the AgNPs dispersion or dispersions with smaller particle size should be tested. The results of this research show that AgNPs are shown to be promising for use as a bactericidal (in-can or in the dry film) in polyurethane coatings, allowing their application in hospitals, food production units, and other environments that require microbial protection.

References

1. Hochmannova, L, Vytrasova, J, "Photocatalytic and Antimicrobial Effects of Interior Paints." *Prog. Org. Coat.*, **67** (1) 1–5 (2010). https://doi.org/10.1016/j.porgcoat.2009.09.016
2. Kumar, A, Vemula, PK, Ajayan, PM, John, G, "Silver-Nanoparticle-Embedded Antimicrobial Paints Based on Vegetable Oil." *Nat. Mater.*, **7** 236–241 (2008)
3. Li, X, Xie, J, Liao, L, Jiang, X, Fu, H, "UV-Curable Polyurethane Acrylate-Ag/TiO₂ Nanocomposites with Superior UV Light Antibacterial Activity." *Int. J. Polym. Mater. Polym. Biomater.*, **66** (16) 835–843 (2017). https://doi.org/10.1080/00914037.2016.1276063
4. Alviano, WS, Alviano, DS, Diniz, CG, Antoniolli, AR, Alviano, CS, Farias, LM, Carvalho, MAR, Souza, MMG, Bolognese, AM, "In Vitro Antioxidant Potential of Medicinal Plant Extracts and Their Activities Against Oral Bacteria Based on Brazilian Folk Medicine." *Arch. Oral Biol.*, **53** (6) 545–552 (2008). https://doi.org/10.1016/j.archoralbio.2007.12.001
5. Rai, M, Yadav, A, Gade, A, "Silver Nanoparticles as a New Generation of Antimicrobials." *Biotechnol. Adv.*, **27** (1) 76–83 (2009). https://doi.org/10.1016/j.biotechadv.2008.09.002
6. Prabhu, S, Poulose, EK, "Silver Nanoparticles: Mechanism of Antimicrobial Action, Synthesis, Medical Applications, and Toxicity Effects." *Int. Nano Lett.*, **2** (1) 32 (2012). https://doi.org/10.1186/2228-5326-2-32
7. de Souza, AV, Valério, A, Buske, JLO, Benedet, ME, Pistor, V, Machado, RAF, "Influence of Stabilizer Additives on Thermochromic Coating for Temperature Monitoring." *J. Coat. Technol. Res.*, **13** (6) 1139–1144 (2016). https://doi.org/10.1007/s11998-016-9811-7
8. Valério, A, Mancusi, E, Ferreira, F, de Souza, SMAGU, González, SYG, "Biopolymer-Hydrophobic Drug Fibers and the Delivery Mechanisms for Sustained Release Applications." *Eur. Polym. J.*, **112** 400–410 (2019). https://doi.org/10.1016/j.eurpolymj.2019.01.016
9. Abd El-Wahab, H, Saleh, TS, Zayed, EM, El-Sayed, AS, Assaker, RSA, "Synthesis and Evaluation of New Antimicrobial Additive Based on Pyrimidine Derivative Incorporated Physically into Polyurethane Varnish for Surface Coating and into Printing Ink Paste." *Egypt. J. Pet.*, **24** (3) 247–253 (2015). https://doi.org/10.1016/j.ejpe.2015.07.002
10. Guardiola, FA, Cuesta, A, Meseguer, J, Esteban, MA, "Risks of Using Antifouling Biocides in Aquaculture." *Int. J. Mol. Sci.*, **13** (2) 1541–1560 (2012). https://doi.org/10.3390/ijms13021541
11. Contant, S, Caritá Júnior, G, Machado, PFMPB, Lona, LMF, "Evaluation of the Effect of Dry-Film Biocides on Paint Film Preservation Using Neural Networks." *Braz. J. Chem. Eng.*, **27** (4) 643–651 (2010). https://doi.org/10.1590/S0104-66322010000400016
12. Kumar, A, Vemula, PK, Ajayan, PM, John, G, "Silver-Nanoparticle-Embedded Antimicrobial Paints Based on

Vegetable Oil." *Nat. Mater.*, **7** (3) 236–241 (2008). https://doi.org/10.1038/nmat2099

13. Ananda, AP, Manukumar, HM, Krishnamurthy, NB, Nagendra, BS, Savitha, KR, "Assessment of Antibacterial Efficacy of a Biocompatible Nanoparticle PC@AgNPs Against *Staphylococcus aureus*." *Microb. Pathog.*, **126** 27–39 (2019). https://doi.org/10.1016/j.micpath.2018.10.029

14. Merchan, M, Sedlarikova, J, Vesel, A, Machovsky, M, Sedlarik, V, Saha, P, "Antimicrobial Silver Nitrate-Doped Polyvinyl Chloride Cast Films: Influence of Solvent on Morphology and Mechanical Properties." *Int. J. Polym. Mater.*, **62** (2) 101–108 (2013). https://doi.org/10.1080/00914037.2012.670821

15. Abou El-Nour, KMM, Eftaiha, A, Al-Warthan, A, Ammar, RAA, "Synthesis and Applications of Silver Nanoparticles." *Arab. J. Chem.*, **3** (3) 135–140 (2010). https://doi.org/10.1016/j.arabjc.2010.04.008

16. Kalishwaralal, K, BarathManiKanth, S, Pandian, SRK, Deepak, V, Gurunathan, S, "Silver Nanoparticles Impede the Biofilm Formation by *Pseudomonas aeruginosa* and *Staphylococcus epidermidis*." *Colloids Surf. B Biointerfaces*, **79** (2) 340–344 (2010). https://doi.org/10.1016/j.colsurfb.2010.04.014

17. Ahmed, S, Ahmad, M, Swami, BL, Ikram, S, "A Review on Plants Extract Mediated Synthesis of Silver Nanoparticles for Antimicrobial Applications: A Green Expertise." *J. Adv. Res.*, **7** (1) 17–28 (2016). https://doi.org/10.1016/j.jare.2015.02.007

18. Kung, J-C, Chen, Y-J, Chiang, Y-C, Lee, C-L, Yang-Wang, Y-T, Hung, C-C, Shih, C-J, "Antibacterial Activity of Silver Nanoparticle (AgNP) Confined Mesoporous Structured Bioactive Powder Against *Enterococcus faecalis* Infecting Root Canal Systems." *J. Non-Cryst. Solids*, **502** 62–70 (2018). https://doi.org/10.1016/j.jnoncrysol.2018.06.030

19. Zhang, X-F, Liu, Z-G, Shen, W, Gurunathan, S, "Silver Nanoparticles: Synthesis, Characterization, Properties, Applications, and Therapeutic Approaches." *Int. J. Mol. Sci.*, **17** (9) 1534 (2016). https://doi.org/10.3390/ijms17091534

20. Jana, NR, Gearheart, L, Murphy, CJ, "Wet Chemical Synthesis of Silver Nanorods and Nanowires of Controllable Aspect Ratio." *Chem. Commun.*, **7** 617–618 (2001). https://doi.org/10.1039/b100521i

21. ASTM, "*ASTM G 154/2004 Standard Practice for Operating Fluorescent Light Apparatus for UV Exposure of Nonmetallic Materials*," 2004. https://doi.org/10.1520/G0154-04

22. ASTM, "*ASTM D 523 Standard Test Method for Specular Gloss*," 2008. https://doi.org/10.1520/D0523-08

23. ASTM, "*ASTM D2574-94 Standard Test Method for Resistance of Emulsion Paints in the Container to Attack by Microorganisms*," 2016

24. ASTM, "*ASTM D 5590 Standard Test Method for Determining the Resistance of Paint Films and Related Coatings to Fungal Defacement by Accelerated Four-Week Agar Plate Assay*," 2017. https://doi.org/10.1520/D5590-17

25. Japanese Standards Association, "*JIS Z 2801:2000 Antimicrobial Products—Test for Antimicrobial Activity and Efficacy*," 2000

26. Jin, R, et al., "Photoinduced Conversion of Silver Nanospheres to Nanoprisms." *Science*, **294** (5548) 1901–1903 (2001). https://doi.org/10.1126/science.1066541

27. Gupta, KK, Jassal, M, Agrawal, AK, "Functional Finishing of Cotton Using Titanium Dioxide and Zinc Oxide Nanoparticles." *Res. J. Text. Appar.*, **11** (3) 1–10 (2007). https://doi.org/10.1108/RJTA-11-03-2007-B001

28. Sundaresan, K, Sivakumar, A, Vigneswaran, C, Ramachandran, T, "Influence of Nano Titanium Dioxide Finish, Prepared by Sol–Gel Technique, on the Ultraviolet Protection, Antimicrobial, and Self-Cleaning Characteristics of Cotton Fabrics." *J. Ind. Text.*, **41** (3) 259–277 (2012). https://doi.org/10.1177/1528083711414962

29. Acharya, D, Mohanta, B, Deb, S, Sen, AK, "Theoretical Prediction of Absorbance Spectra Considering the Particle Size Distribution Using Mie Theory and Their Comparison with the Experimental UV–Vis Spectra of Synthesized Nanoparticles." *Spectrosc. Lett.*, **51** (3) 139–143 (2018). https://doi.org/10.1080/00387010.2018.1442351

30. Freitas, C, Müller, RH, "Effect of Light and Temperature on Zeta Potential and Physical Stability in Solid Lipid Nanoparticle (SLN^{TM}) Dispersions." *Int. J. Pharm.*, **168** (2) 221–229 (1998). https://doi.org/10.1016/S0378-5173(98)00092-1

31. Valério, A, Conti, DS, Araújo, PHH, Sayer, C, da Rocha, SRP, "Synthesis of PEG–PCL-Based Polyurethane Nanoparticles by Miniemulsion Polymerization." *Colloids Surf. B Biointerfaces*, **135** 35–41 (2015). https://doi.org/10.1016/j.colsurfb.2015.07.044

32. Tantra, R, Schulze, P, Quincey, P, "Effect of Nanoparticle Concentration on Zeta-Potential Measurement Results and Reproducibility." *Particuology*, **8** (3) 279–285 (2010). https://doi.org/10.1016/j.partic.2010.01.003

33. Campoccia, D, Montanaro, L, Arciola, CR, "A Review of the Biomaterials Technologies for Infection-Resistant Surfaces." *Biomaterials*, **34** (34) 8533–8554 (2013). https://doi.org/10.1016/j.biomaterials.2013.07.089

34. Panáček, A, Kolář, M, Večeřová, R, Prucek, R, Soukupová, J, Kryštof, V, Hamal, P, Zbořil, R, Kvítek, L, "Antifungal Activity of Silver Nanoparticles Against *Candida* spp." *Biomaterials*, **30** (31) 6333–6340 (2009). https://doi.org/10.1016/j.biomaterials.2009.07.065

35. dos Santos, CA, Jozala, AF, Pessoa, A, Jr, Seckler, MM, "Antimicrobial Effectiveness of Silver Nanoparticles Co-stabilized by the Bioactive Copolymer Pluronic F68." *J. Nanobiotechnol.*, **10** (1) 43 (2012). https://doi.org/10.1186/1477-3155-10-43

36. Perito, B, Giorgetti, E, Marsili, P, Muniz-Miranda, M, "Antibacterial Activity of Silver Nanoparticles Obtained by Pulsed Laser Ablation in Pure Water and in Chloride Solution." *Beilstein J. Nanotechnol.*, **7** 465–473 (2016). https://doi.org/10.3762/bjnano.7.40